Parameter Identification for Planetary Soil Based on a Decoupled Analytical Wheel-Soil Interaction Terramechanics Model

Liang Ding, Kazuya Yoshida, Keiji Nagatani, Haibo Gao and Zongquan Deng

Abstract—**Identifying planetary soil parameters is not only an important scientific goal, but also necessary for exploration rover to optimize its control strategy and realize high-fidelity simulation. An improved wheel-soil interaction mechanics model is introduced, and it is then simplified by linearizing the normal stress and shearing stress to derive closed-form analytical equations. Eight unknown soil parameters are divided into three groups. The highly complicated coupled equations, each of which includes all the unknown soil parameters, are then decoupled. Each decoupled equation contains one or two groups of soil parameters, making it feasible to make a step-by-step identification of all the unknown parameters that characterize the soil. Wheel-soil interaction experiments were performed for six kinds of wheels with different dimensions and wheel lugs on simulated planetary soil. Soil parameters are identified with the measured data to validate the method, which are then used to predict wheel-soil interaction forces and torque, with a less than 10% margin of error. The improved model, decoupled analytical model, and soil-characterizing method can play important roles in the development of both the planetary exploration rovers and the terrestrial vehicles.**

I. Introduction

SCIENTISTS have long been interested in the soil mechanics properties of planetary rovers, both to improve our scientific knowledge of the geological properties of planetary soil and to provide engineering knowledge required to perform planetary surface exploration or future settlement activities.

During the lunar exploration missions carried out in the 1970s, the U.S.A. and the former Soviet Union brought soil samples back to the earth and conducted research on their properties [1]. Due to a lack of samples obtained from a return mission, the more recent exploration of Mars and the moon has required soil research to be conducted remotely. Compared to the research on samples that have been brought back, the in-situ research on soil mechanics properties is low in cost, and it can conveniently be conducted at any time or place with little influence on the original mechanical properties of the soil.

Viking Lander performed soil experiments by scraping the soil to dig trenches with a surface sampling arm. The internal cohesion and friction angles of different types of soils (drift, crusty and cloddy) were estimated [2]. W. Hong developed a system for estimating soil properties in-situ using a manipulator arm, including soil mechanics modeling and estimation techniques [3]. Researchers from the Sojourner rover team conducted experiments by driving one wheel on the rover while keeping the other wheels stationary. The soil appeared to show little or no cohesion, and the friction angles were found to be between 32° and 41° [4]. Mechanical experiments were also performed during NASA Mars Exploration Rover Missions [5]. The Spirit and Opportunity rovers researched the soil properties of Meridiani Planum [6] and Gusev Crater [7], respectively, by excavating the subsurface soil with wheels for in-situ observation, studying the rock mechanical properties with a rock abrasion tool and analyzing the wheel track patterns, depths, and wheel slippage dynamics during traverses.

Wheel-soil interaction terramechanics models consist of not only the internal cohesion and friction angle of the soil but also many other parameters such as the cohesive modulus, friction modulus, and sinkage exponent, which can express the pressure bearing capability of soil [8]. This makes it possible to characterize planetary soil more comprehensively by estimating soil parameters according to the forces and moments that act upon the wheel. In addition, for future rover-based exploration missions conducted on more challenging terrains, such as the MSL and ExoMars missions for exploring Mars and the SELENE and Chang'e lunar rover plans, the rover must know the variations in soil parameters in time to optimize its control and planning strategy. This enables it to maximize wheel traction or minimize power consumption [9] as well as update the parameters for rover simulation on Earth, a boon to the successful achievement of scientific goals. Two important issues, however, must first be resolved in regard to wheel-soil interaction mechanics based parameter identification. One issue is the development of a high-fidelity wheel-soil interaction terramechanics model for planetary rovers. The other issue is to simplify the relevant complex coupled nonlinear integrated equations in order to obtain simple closed-form equations.

The classical terramechanics models for terrestrial vehicles are usually used for planetary rovers [8], [10], [11]. K.

This work was supported by National High Technology Research and Development Program of China (grant No. 2006AA04Z231), Key Natural Science Foundation of Heilongjiang Province in China (grant No. ZJG0709) and Foundation of Chinese State Key Laboratory of Robotics and Systems (grant No. SKLRS200801A02).

L. Ding, K. Yoshida, and K. Nagatani are with the Department of Aerospace Engineering, Tohoku University, Aoba 6-6-01, Sendai, 980-8579, Japan (e-mail: {liangding, yoshida}@astro.mech.tohoku.ac.jp, keiji@ieee.org).

L. Ding, H. Gao and Z. Deng are with School of Mechatronics Engineering, Harbin Institute of Technology, Harbin 150001, Heilongjiang, China; State Key Laboratory of Robotics and System (HIT), Harbin 150001, Heilongjiang, China (e-mail: gaohaibo@hit.edu.cn, dengzq@hit.edu.cn).

Iagnemma et al. linearized the Wong-Reece normal stress equation and Janosi shearing stress equation in order to obtain a closed-form formula, and then, they applied a linear least-squares estimator in order to estimate the internal cohesion and friction angle online by setting the shearing deformation modulus to a typical value [12]. This method is used to estimate the terrain for planetary rovers so that they can adapt their control strategies and maximize effectiveness [13]. S. Hutangkabodee et al. developed a method to identify the internal friction angle, shearing deformation modulus, and lumped pressure sinkage coefficient (cohesive sinkage modulus and frictional sinkage modulus), while the internal cohesion was fixed to 3 Kpa. The composite Simpson's rule was employed to obtain an approximated form model [14].

The fidelity of wheel-soil interaction models can determine the precision of parameter identification. An improved model for calculating the interaction mechanics was developed that took into account the slip-sinkage and lug effect, which gave considerable precision to the prediction of both the mechanics and the entire sinkage of the wheel [15], a subject that is introduced in Section II. Section III deduces a decoupled closed-form analytical formula, which is then used to predict eight soil parameters in Section IV. Section V describes the experimental study of wheel-soil interaction mechanics; the data obtained are used for parameter identification to validate the above algorithm in Section VI.

II. WHEEL-SOIL INTERACTION MECHANICS MODEL

A. General model for lugged planetary wheel

Planetary rovers are usually installed with lugs of a certain height to improve their tractive ability in deformable soil. Fig. 1 shows a diagram of lugged wheel-soil interaction mechanics [12], where z is the wheel sinkage; θ_1, the entrance angle at which the wheel begins to contact the soil; θ_2, the exit angle at which the wheel looses contact with the soil; θ_m, the angle of maximum stress; θ_1', the angle where the soil begins to deform; W, the vertical load of the wheel; DP, the resistance provided by forward movement, which is equal to the drawbar pull; T, the driving torque of the motor; r, the wheel radius; h, the height of the lugs; v, the vehicle velocity; and ω, the angular velocity of the wheel. The soil interacts with the wheel in the form of continuous normal stress σ and shearing stress τ, which are divided into a forward part (σ_1, τ_1) and a rear part (σ_2, τ_2).

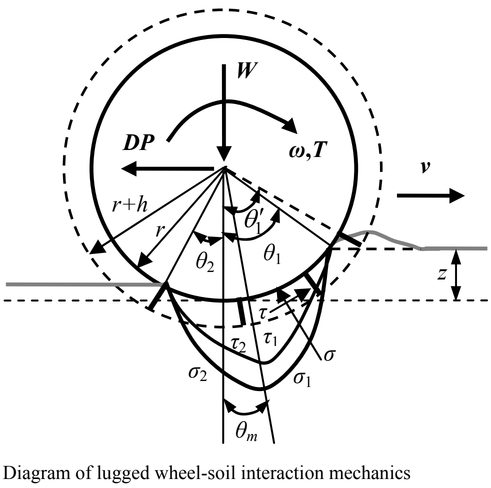

Fig.1 Diagram of lugged wheel-soil interaction mechanics

For a steadily moving wheel, force balance equations can be expressed by integrating the stresses as follows:

$$\begin{cases} W = b\{\int_{\theta_2}^{\theta_m}[r\sigma_2(\theta)\cos\theta + r_s\tau_2(\theta)\sin\theta]d\theta + \\ \quad \int_{\theta_m}^{\theta_1}[r\sigma_1(\theta)\cos\theta + r_s\tau_1(\theta)\sin\theta]d\theta\} \\ DP = b\{\int_{\theta_2}^{\theta_m}[r_s\tau_2(\theta)\cos\theta - r\sigma_2(\theta)\sin\theta]d\theta + \\ \quad \int_{\theta_m}^{\theta_1}[r_s\tau_1(\theta)\cos\theta - r\sigma_1(\theta)\sin\theta]d\theta\} \\ T = r_s^2 b[\int_{\theta_2}^{\theta_m}\tau_2(\theta)d\theta + \int_{\theta_m}^{\theta_1}\tau_1(\theta)d\theta] \end{cases} \tag{1}$$

where b is the width of the wheel, r_s is the equivalent shearing radius, i.e., the average radius where the shearing between the moving soil adhered to the wheel and static soil takes place:

$$r_s = r + \lambda_s h \qquad (0 \le \lambda_s \le 1) \tag{2}$$

The lug coefficient λ_s in (2) is related to the internal friction angle of the soil and the number of lugs, and it is set to 0.5 for the purpose of simplification [16].

B. Normal stress and shearing stress distribution

Let s denote the slip ratio, an important state variable of wheel soil interaction. It is defined with r_s [16]:

$$s = \begin{cases} (r_s\omega - v)/r_s\omega & (r_s\omega \ge v, 0 \le s \le 1) \\ (r_s\omega - v)/v & (r_s\omega < v, -1 \le s < 0) \end{cases} \tag{3}$$

The normal stress equation is improved on the basis of the Wong-Reece model [15]:

$$\begin{cases} \sigma_1(\theta) = (\frac{k_c}{b} + k_\phi)r^N(\cos\theta - \cos\theta_1)^N & (\theta_m \le \theta \le \theta_1) \\ \sigma_2(\theta) = (\frac{k_c}{b} + k_\phi)r^N\{\cos[\theta_1 - \frac{\theta - \theta_2}{\theta_m - \theta_2}(\theta_1 - \theta_m)] - \cos\theta_1\}^N \\ (\theta_2 \le \theta < \theta_{\mathrm{m}}) \end{cases} \tag{4}$$

where k_c is the cohesive modulus of the soil, k_φ is the frictional modulus, and N is the improved soil sinkage exponent. N is the linear function of the slip ratio:

$$N = n_0 + n_1 s \tag{5}$$

where n_0 and n_1 are coefficients for calculating N. Equation (5) is deduced to change the constant sinkage exponent n with the slip ratio to predict all sinkage of the wheel, including severe slip sinkage [17], which cannot be reflected well by the conventional model. The sinkage exponent N is an increasing function of the slip ratio, while the normal stress is a decreasing function of N. Therefore, the entrance angle and sinkage increase as the slip ratio increases. The linearized method is effective in predicting wheel slip sinkage.

Angles θ_1, θ_2, and θ_m are functions of wheel sinkage z and coefficients c_1 c_2 and c_3:

$$\theta_1 = \mathrm{acos}[(r - z)/r] \tag{6}$$

$$\theta_m = (c_1 + c_2 s)\theta_1 \tag{7}$$

$$\theta_2 = c_3\theta_1 \quad (8)$$

The leaving angle θ_2 is usually simplified as zero, as is the parameter c_3.

The Janosi equation for calculating shearing stress was also improved [15]:

$$\begin{aligned}\tau(\theta) = &[c+\sigma(\theta)\tan\phi]\times \\ &\{1-\exp(-r_s[(\theta_1'-\theta)-(1-s)(\sin\theta_1'-\sin\theta)]/k)\}\end{aligned} \quad (9)$$

where c is the cohesion of the soil, φ is the internal friction angle, and k is the shearing deformation modulus.

$$\theta_1' = \text{acos}\left[(r-z)/R_j\right] \quad (10)$$

$$R_j = \begin{cases} r+h & (0 \le s \le s_{j1}) \\ r+h(s_{j2}-s)/(s_{j2}-s_{j1}) & (s_{j1} < s < s_{j2}) \\ r & (s_{j2} \le s \le 1) \end{cases} \quad (11)$$

If the entrance angle is θ_1 and wheel sinkage is small (indicated by a slip ratio less than approximately 0.15), soil displacement can be considered as starting from angle θ_1' calculated by the maximum radius $r + h$ (as shown in Fig. 1). If wheel sinkage is great, the next lug cannot contact the soil immediately after the former one completely enters the soil. The interaction between lug and soil is quite a complex process. The radius R_j for calculating θ_1' is deduced in order to approximate the effect of that process. Transitional slip ratios s_{j1} and s_{j2} are adopted because wheel sinkage is related to the slip ratio [15]. If the slip ratio is larger than 0.5, the influence of wheel lugs on the starting angle of soil deformation can be ignored. According to the above analysis, the parameters s_{j1} and s_{j2} are 0.15 and 0.5 respectively.

Equations (5) and (10) contribute most to the improvement of the model, as they reflect wheel slip-sinkage phenomena and the lug effect quite well. More details can be found in [15].

Apart from λ_s, c_3, s_{j1}, and s_{j2}, which have been determined, there remain nine unknown soil parameters: c_1, c_2, k_c, k_φ, n_0, n_1, c, φ, and k.

III. Decoupled Analytical Model Derivation

A. Model Analysis

The wheel-soil interaction model in (1) includes three equations. Given s and θ_1, W, DP and T can be calculated if the soil parameters are known. Figure 2 shows the process. Inversely, if W, DP, T, and θ_1 of different slip ratios are measured, it is possible to identify the unknown soil parameters by means of the data fitting method. However, the equations are highly coupled, and each of them contains all the unknown parameters. It is not feasible, therefore, to identify these nine parameters simultaneously by means of the measured data, due to the complexity and high nonlinearity of the model, which can easily lead to local convergence.

Let $K_s = K_c/b + K_\varphi$ denote the wheel-soil interaction sinkage exponent, i.e., the lumped pressure-sinkage coefficient in [14]. For a wheel of a certain width b, the parameter K_s is constant. K_s will therefore replace k_c and k_φ, which are not feasible and don't need to be separately identified. The parameters can be divided into three groups: $P_{\text{I}} = \{c_1, c_2,\}$, $P_{\text{II}} = \{K_s, n_0, n_1\}$, $P_{\text{III}} = \{c, \varphi, k\}$, which are directly related to angles of θ_m and θ_2, normal stress and shearing stress, respectively.

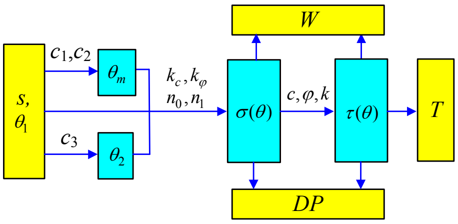

Fig. 2 Diagram of coupled wheel-soil interaction mechanics model

If the equations can be decoupled to separate the variables of three groups, it will become easier, and feasible, to identify all the unknown parameters.

B. Stress Simplification

Let σ_m denote the maximum normal stress, and τ_m denote the maximum shearing stress:

$$\sigma_m = K_s r^N (\cos\theta_m - \cos\theta_1)^N \quad (12)$$

$$\begin{aligned}\tau_m = &(c+\sigma_m\tan\phi)\times \\ &(1-\exp\{-r_s[(\theta_1'-\theta_m)-(1-s)(\sin\theta_1'-\sin\theta_m)]/k\})\end{aligned} \quad (13)$$

The normal stress and shearing stress can be simplified by means of the linearized method [12]:

$$\begin{cases}\sigma_1(\theta) \approx \sigma_1^L(\theta) = \sigma_m(\theta_1-\theta)/(\theta_1-\theta_m) & (\theta_m \le \theta \le \theta_1) \\ \sigma_2(\theta) \approx \sigma_2^L(\theta) = \sigma_m(\theta-\theta_2)/(\theta_m-\theta_2) & (\theta_2 \le \theta < \theta_{\text{m}})\end{cases} \quad (14)$$

$$\begin{cases}\tau_1(\theta) \approx \tau_1^L(\theta) = \tau_m(\theta_1-\theta)/(\theta_1-\theta_m) & (\theta_m \le \theta \le \theta_1) \\ \tau_2(\theta) \approx \tau_2^L(\theta) = \tau_m(\theta-\theta_2)/(\theta_m-\theta_2) & (\theta_2 \le \theta < \theta_{\text{m}})\end{cases} \quad (15)$$

The literature [12] has verified the linearized method for soils with a sinkage exponent in the range of 0.5 to 1.6. Soil exponent sinkage influences the simplification error. Six kinds of wheels (Section V) with wheel-soil interaction exponent coefficients n_0 and n_1 [15] close to the identified value (Section VI) are used to check the error. Three groups of typical values are selected: $\theta_1 = 35°$, $s = 0.4$; $\theta_1 = 25°$, $s = 0.2$; $\theta_1 = 15°$, $s = 0$, which are comparable to the experimental results of wheel-soil interaction presented in Section V. The results of calculations show that the maximum relative error is larger for a lower slip ratio because the sinkage exponent is smaller. The maximum simplification error for both normal stress and shearing stress is approximately 15%.

C. Closed-form analytical equations

By substituting (14) and (15) for (1) and integrating the equations, one arrives at:

$$\begin{bmatrix} W \\ DP \\ T \end{bmatrix} = \begin{bmatrix} A & B \\ -B & A \\ 0 & r_s C \end{bmatrix} \begin{bmatrix} X \\ Y \end{bmatrix} \quad (16)$$

where $A = \dfrac{\cos\theta_m - \cos\theta_2}{\theta_m - \theta_2} + \dfrac{\cos\theta_m - \cos\theta_1}{\theta_1 - \theta_m}$, $X = rb\sigma_m$,

$B = \dfrac{\sin\theta_m - \sin\theta_2}{\theta_m - \theta_2} + \dfrac{\sin\theta_m - \sin\theta_1}{\theta_1 - \theta_m}$, $Y = r_s b\tau_m$, $C = \dfrac{\theta_1 - \theta_2}{2}$.

A, B and, C are functions of entrance angle θ_1 and parameters of P_{I}, X is related to parameters of P_{I} and P_{II}, while

Y is related to all parameters. It is clear that W, DP and T are functions of all the soil parameters.

D. Decoupling of equations

According to (16),

$$X = (W - BY)/A = (AY - DP)/B \quad (17)$$

$$Y = T/(r_s C) \quad (18)$$

By substituting (17) and (18) into (16), one obtains:

$$DP = AY - B\frac{W - BY}{A} = \frac{A^2 + B^2}{r_s AC}T - \frac{B}{A}W \quad (19)$$

$$W = AX + BT/(r_s C) = rbA\sigma_m + BT/(r_s C) \quad (20)$$

According to (20),

$$\sigma_m = W/(rbA) - BT/(rr_s bAC) \quad (21)$$

Let $D = 1 - \exp\{-r_s[(\theta_1' - \theta_m) - (1-s)(\sin\theta_1' - \sin\theta_m)]/k)\}$. Substitute $Y = r_s b\tau_m$, Eqs. (13) and (21) in (16), and one obtains:

$$T = r_s^2 CD\{bc + [W/(rA) - BT/(rr_s AC)]\tan\varphi\} \quad (22)$$

The explicit formulation of T is:

$$T = r_s^2 CD[bc + W\tan\varphi/(rA)]/[1 + r_s BD\tan\varphi/(rA)] \quad (23)$$

Equations (19), (20) and (23) are decoupled equations. DP is the function of the parameters in P_{I}; W is the function of the parameters in P_{I} and P_{II}; while T is the function of the parameters in P_{I} and P_{III}.

IV. Parameter Identification Method

A. Identifying c_1 and c_2

According to (19), DP is the function of W, T, θ_1, s and the unknown parameters c_1 and c_2. c_1 and c_2 can be identified if the other parameters have been measured, as shown in Fig. 3.

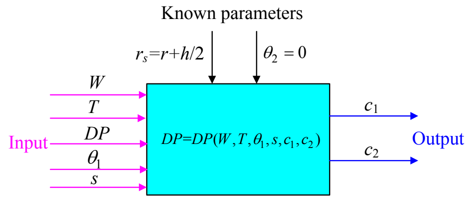

Fig.3 Diagram for identifying c_1 and c_2

W, T, s, and θ_1 of the rover can be measured or estimated [12]. The entrance angle θ_1 can be measured by visual means or by kinematic analysis of the rover's suspension. The vertical load W can be estimated by quasi-static force analysis. The torque T can be estimated by reference to the current of the motor as measured by its driver. The wheel angular speed ω can be measured with an encoder. The wheel longitudinal velocity v can be measured in terms of inertial measurement units (IMU) or visual odometry. Knowing v and ω, the slip ratio can be estimated with (3). The drawbar pull can be measured by installing a force sensor on the wheel, but this may cause extra complexity and expense. Quasi-static analysis can also help in estimating the drawbar pull. The slip ratio of a wheel can be changed by modulating the velocity of different wheels.

B. Identifying K_s, n_0 and n_1

According to (12) and (20),

$$F_N = rbA[K_s r^{n_0+n_1 s}(\cos\theta_m - \cos\theta_1)^{n_0+n_1 s}] + BT/(r_s C) \quad (24)$$

As shown in Fig. 4, three parameters K_s, n_0 and n_1 can be identified according to the measured θ_1, W, T, s and identified c_1, c_2.

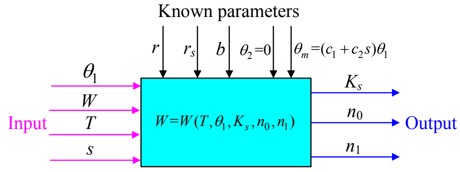

Fig.4 Diagram for identifying K_s, n_0 and n_1

C. Identifying c, φ and k

By substituting the values of D in (23), one obtains:

$$T = \frac{r_s^2 C[bc + W\tan\varphi/(rA)] \times (1 - \exp\{-r_s[(\theta_1' - \theta_m) - (1-s)(\sin\theta_1' - \sin\theta_m)]/k)\})}{1 + [r_s B\tan\varphi/(rA)] \times (1 - \exp\{-r_s[(\theta_1' - \theta_m) - (1-s)(\sin\theta_1' - \sin\theta_m)]/k)\})} \quad (25)$$

As shown in Fig. 5, parameters c, φ, and k can be identified with the measured θ_1, W, T, and s with (25).

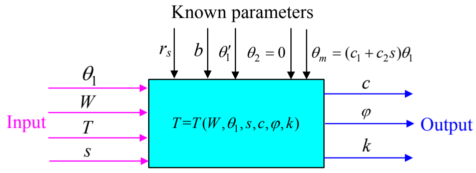

Fig.5 Diagram for identifying c, φ and k

D. Parameter identification implementation

The least square method is adopted to identify the soil parameters with the *lsqcurvefit()* function of Matlab. Let x denote the vector of identified parameters, $xdata$ denote slip ratio as the input data, $ydata$ denote the measured DP, W and T, m denote the length of $xdata$ and $ydata$, and F denote the function of (19), (24) and (25) respectively. The identifying process seeks to find the vector x that best fits (26):

$$\min_x \frac{1}{2}\|F(x, xdata) - ydata\| = \frac{1}{2}\sum_{i=1}^{m}[F(x, xdata_i) - ydata_i]^2 \quad (26)$$

V. Experimental Study of Wheel-Soil Interaction

A. Experimental equipment and materials

Figure 6 shows the wheel-soil interaction testbed that was used to perform the experiments. The testbed consists of three motors and various related sensors. The driving motor can cause the wheel to move forward; the carriage motor is used together with a conveyance belt to imitate the influence of the vehicle body on the wheel and to create various slip ratios; and the steering motor is used for research into steering. Wheel sinkage z is measured by a high precision sliding resistance displacement sensor; T, DP and W can be measured with a torque sensor and F/T sensor.

The design of the experimental wheels was based upon those in recent planetary rovers (Fig. 7). Six types of cylindri-

Fig.6 Wheel-soil interaction test bed and experimental wheel

cal metal wheels with different radii, widths and lugs were used, as shown in Table I, where n_L is the number of wheel lugs.

TABLE I
PARAMETERS OF EXPERIMENTAL WHEELS

Test No.	Wheel code	r(mm)	b(mm)	h(mm)	n_L
T1	Wh11	135	165	15	24
T2	Wh12	135	165	10	24
T3	Wh21	135	110	15	24
T4	Wh22	135	110	10	24
T5	Wh31	157.35	165	15	30
T6	Wh32	157.35	165	10	30

The literature shows that the mechanical properties of dry loose sand are similar to those of planetary soil, so that such sand is usually employed as planetary soil simulant. The simulant used in this study was made from soft sand after removal of impurities, sieving, ventilating and drying. The soil parameters measured by means of plate sinkage and shearing experiments are sinkage exponent $n = 1.10$, cohesive modulus of sinkage $k_c = 15.6$ Kpa/m^{n-1}, frictional modulus of sinkage $k_\varphi = 2407.4$ KPa/m^n; internal cohesion of the soil $c = 251$ Pa, and friction angle $\varphi = 31.9°$ [15].

B. Experiment Setup

The forward velocity of wheel was 10 mm/s. The experimental slip ratios were 0, (0.05), 0.1, 0.2, 0.3, 0.4, (0.5), and 0.6. The slip ratios were calculated with $\lambda_s = 1$, and the values were amended with the shearing radius r_s [16]. The vertical wheel load was approximately 80 N. All the setting values were comparable to those of planetary rovers.

C. Results

Hundreds of raw data could be obtained for a single test. The measured data fluctuate periodically in correspondence with the entrance and exit of the wheel lugs. The results of the experiment show that the mean values of several tests are almost the same, regardless of fluctuations in the data. The wheel interacted with the soil to achieve a steady state after it was kept running for several seconds. The steady data were used in order to calculate the mean values of z, DP, W and T after filtering. The entrance angles were then calculated with the wheel sinkage. The curves of θ_1, DP, W, and T versus slip ratio were obtained for the 6 kinds of wheels used.

VI. EXPERIMENTAL VERIFICATION

A. Parameter identification result and discussion

Experimental data were used to identify the soil parameters. Table II shows the results (the unit of K_s is Kpa/m^N) and Table III shows the data fitting error and calculation time.

The data fitting result of Wh11 is plotted in Fig. 7 (M1). The relative data fitting error values for DP, W and T are smaller than 4.13%. The computation time for fitting DP and W is smaller than 50 ms on a 2G Hz laptop PC, but it sometimes takes about 150 ms to fit T due to the complexity

TABLE II
IDENTIFIED SOIL PARAMETERS

Wheel code	W11	W12	W21	W22	W31	W32
c_1	0.504	0.381	0.531	0.415	0.486	0.371
$-c_2$	0.377	0.228	0.299	0.038	0.308	0.090
K_s	2498.9	2499.2	2499.2	2499.6	2515.6	2499.2
n_0	0.767	0.864	0.820	0.915	0.727	0.806
n_1	1.336	1.094	1.136	0.840	1.332	1.148
c (Pa)	95.5	199.0	284.8	239.1	204.6	217.1
φ (°)	32.2	29.1	31.3	29.4	30.8	28.8
K(mm)	13.1	11.5	12.7	10.6	11.2	9.7

TABLE III
DATA FITTING ERROR AND CALCULATION TIME

Wheel code	Relative error			Calculation time		
	DP(%)	W(%)	T(%)	DP(ms)	W(ms)	T(ms)
W11	2.88	1.62	3.86	19.83	21.864	103.83
W12	3.14	1.05	1.03	15.44	22.752	12.73
W21	2.20	0.70	1.30	21.61	23.931	161.63
W22	2.68	0.94	0.56	15.98	21.455	144.97
W31	4.13	3.60	3.70	19.88	45.598	50.60
W32	3.70	1.07	2.16	13.99	21.675	13.52

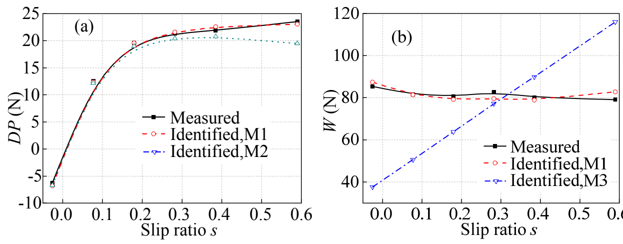

Fig.7 Data fitting result for DP and W of Wh11

of (25). The calculation time can be decreased by optimizing the codes and further simplifying (25). In any case, it can be concluded that this method is suitable for online planetary soil parameter identification.

The largest error for identified φ is only 3.1°. The error of c is also very small as compared to the shearing stress; a difference of only several Kpa. Parameter k has an acceptable range from 9.7 mm to 13.1 mm. Parameter K_s is sensitive to the initial value and the identified result is quite close to the initial value 2500 Kpa/m^N, meaning that only n_0 and n_1 are sufficient for fitting the vertical load. K_s could be fixed to the value of estimated soil frictional modulus k_φ, as k_c is so small as to be negligible [12]. For example, for lunar soil, K_s can be set to $k_\varphi = 820$ Kpa/m^N by ignoring $k_c = 1.4$ Kpa/m^{N+1}. The bearing performance of soil could be quite well characterized by the identified n_0 and n_1. The range of $n_0 + n_1 s$ for the experimental planetary soil stimulant is from 0.73 (W31, $s = 0$) to 2.10 (W11, $s = 1$), from which wheel sinkage into the soil can be estimated.

Parameter c_1 is between 0.37 and 0.53, while c_2 is between –0.38 and –0.04. Their values exhibit a wide range, but the other identified parameters are not obviously influenced by this. This means that wheel-soil interaction mechanics are not sensitive to c_1 and c_2. One can therefore assign typical values of c_1 and c_2 to the soil even if the values of *DP* are unknown. If we let $c_1 = 0.5$ and $c_2 = 0$, the drawbar pull can be fitted with an acceptable maximum relative error of 8.57% (M2 in Fig. 7 (a)), the data fitting error or *W* and *T*, and the identification results of the other parameters are not significantly influenced.

If a constant sinkage exponent is used instead of *N* in (5), the identification results for Wh11 are $K_s = 14.2$ Kpa/m^n and $n = 0$ (lower limit). The fitting errors of *W* are quite large (M3 in Fig.7 (b)). Extending the limits of *n*, the best data fitting result for K_s is from 1.32 Kpa/m^n (Wh11) to 2.66 Kpa/m^n (Wh11), *n* is from –0.54 (Wh11) to –0.50 (Wh31), which is far from the soil parameters. If (10) is not used, i.e., the influence of lugs on the starting angle of soil deformation is ignored, then the identified *c* ranges from 448 Pa (Wh12) to 3071 Pa (Wh11), φ from 15.7° (Wh11) to 26.2° (Wh12), and *k* from 1.3 mm (Wh31) to 5.5 mm (Wh12). These results, however, are untenable, and the fitting error of *T* reaches 10.58% (Wh31).

B. Mechanics prediction with identified parameters

The prediction of wheel-soil interaction mechanics by means of the identified parameters can be applied to rover design, control strategy optimization, and dynamics simulation.

The process for mechanics prediction is as follows. (1) Given the vertical load W_a (the average value of measured *W*, 80~85N), slip ratio *s,* and the initial value of the entrance angle. (2) Calculate σ_m and τ_m with (12) and (13). (3) Calculate *W* with (16). (4) If $|W - W_a| > \delta$ (error tolerance), change θ_1 and return to (2); or else, calculate *z*. (5) Calculate *DP* and *T* with (16).

Table IV shows the relative error and calculation time. The maximum relative error for *z*, *DP* and *T* are 1.89%, 9.09% and 4.28%, respectively. The calculation time for *z* is less than 30 ms and that for *DP* and *T* is about 30 μs. These are feasible values for real-time application.

TABLE IV
WHEEL-SOIL INTERACTION MECHANICS PREDICTION ERROR AND TIME

Wheel code	Relative error			Calculation time	
	z (%)	*DP* (%)	*T* (%)	*z* (ms)	*DP* and *T* (μs)
W11	1.15	4.97	2.20	25.313	33
W12	1.71	5.46	1.73	28.872	31
W21	1.09	5.44	3.00	27.771	31
W22	1.13	9.09	2.54	27.553	33
W31	1.89	8.94	4.28	29.640	33
W32	0.79	7.58	1.37	27.274	31

VII. CONCLUSION

The improved model is effective and superior to the original model. The closed-form analytical equations for calculating *DP*, *W*, and *T* are suitable for real-time applications because of their high precision and short calculation time. It is possible to characterize planetary soil more comprehensively with the decoupled analytical model onboard, which can help us better understand planetary soil. The methods and results developed in this study can also be extended to terrestrial wheeled vehicles and mobile robots. Our results also suggest that a new kind of soil parameter measurement meter based on wheel-soil interaction mechanics should be developed.

REFERENCES

[1] W. D. Carrier, G. R. Olhoeft, and W. Mendell, “Physical properties of the lunar surface,” In *Lunar Source Book*, G. H. Heiken, D. T. Vaniman, B. M. French, Eds. New York: Cambridge Univ., 1991, pp. 475-594.

[2] H. J. Moore, G. D. Clow, and R. E. Hutton, “A summary of Viking sample trench analyses for angles of internal friction and cohesion,” *Journal of Geophysical Research*, Vol. 87, pp. 10043-10050, 1982.

[3] The Rover Team, “Characterization of the Martian surface deposits by the Mars pathfinder rover, sojourner,” *Science*, vol. 278, no.5344, pp. 1765-1768, December, 1997.

[4] W. Hong, “Modeling, estimation, and control of robot-soil interactions,” Ph.D. dissertation, Dept. Mech. Eng., Massachusetts Institute of Technology, Cambridge, MA, 2001.

[5] R. E. Arvidson, R. C. Anderson, A. F. C. Haldemann, G. A. Landis, R.Li *et al*. “Physical properties and localization investigations associated with the 2003 Mars Exploration rovers,” *J. Geophys. Res.*, vol. 108(E12), pp. 8070, Oct. 2003.

[6] R.E. Arvidson, R.C. Anderson, P. Bartlett, J.F. Bell, D. Blaney *et al.* “Localization and physical properties experiments conducted by Spirit at Gusev Crater,” *Science*, vol. 305, no. 5685, pp. 821-82, Aug. 2004.

[7] R.E. Arvidson, R.C. Anderson, P. Bartlett, J.F. Bell, P. R. Christensen *et al*. “Localization and physical property experiments conducted by Opportunity at Meridiani Planum,” *Science*, vol. 306. no. 5702, pp. 1730–1733, Dec. 2004.

[8] G. Bekker, *Introduction to Terrain-Vehicle Systems*. Ann Arbor, MI: Univ. of Michigan Press, 1969.

[9] K. Iagnemma and S. Dubowsky, “Mobile robot rough-terrain control (RTC) for planetary exploration,” in *Proc. 26th ASME Biennial Mechanisms and Robotics Conf*., Baltimore, MD, 2000.

[10] J. Y. Wong and A. R. Reece, “Prediction of rigid wheel performance based on analysis of soil-wheel stresses, part I: performance of driven rigid wheels,” *J. Terramechanics*, vol. 4, no.1, pp. 81–98, Jan. 1967.

[11] Z. Janosi and B. Hanamoto, “Analytical determination of drawbar pull as a function of slip for tracked vehicle in deformable soils,” in *Proc. 1st Int. Conf. of ISTVES*, Torino, Italy, 1961, pp. 707-726.

[12] K. Iagnemma, S. Kang, H. Shibly, and S. Dubowsky, “Online terrain parameter estimation for wheeled mobile robots with application to planetary rovers,” *IEEE Transactions on Robotics*, vol. 20, no. 5, pp. 921-927, Oct. 2004.

[13] K. Iagnemma, S. Kang, C. Brooks, and S. Dubowsk, “Multi-sensor terrain estimation for planetary rovers,” in *Proc. 7th Int. Symp. Artif. Intelligence, Robotics and Automation in Space*, Nara, Japan, 2003.

[14] S. Hutangkabodee, Y. H. Zweiri, L. D. Seneviratne, and K. Althoefer, “Performance prediction of a wheeled vehicle on unknown terrain using identified soil parameters,” in *Proc. 2006 IEEE Int. Conf. on Robotics and Automation*, Orlando, FL, 2006, pp. 3356-3361.

[15] L. Ding, H. Gao, Z. Deng, K. Yoshida and K. Nagatani, “Wheel-soil interaction mechanics model for planetary rover on loose soil considering lug effect and slip-sinkage,” *Journal of ASME Applied Mechanics*, to be submitted for publication.

[16] L. Ding, H. Gao, Z. Deng, K. Yoshida and K. Nagatani, “Slip ratio for lugged wheel of planetary rover in deformable soil: definition and estimation,” in *Proc. 2009 IEEE/RSJ Int. Conf. Intelligent Robots and Systems*, St. Louis, MO.

[17] L. Ding, H. Gao, Z. Deng, and J. Tao, “Wheel slip-sinkage and its prediction model of lunar rover,” *Journal of Central South University of Technol*ogy, in press.